Enhancing corrosion and biofouling resistance through superhydrophobic surface modification

P. V. Mahalakshmi, S. C. Vanithakumari, Judy Gopal, U. Kamachi Mudali* and Baldev Raj

Corrosion Science and Technology Group, Indira Gandhi Centre for Atomic Research, Kalpakkam 603 102, India

A simple approach was developed for generating superhydrophobic surface modification of titanium and 9Cr-1Mo steel. Motivated by the lotus effect in which water droplets falling on the leaves bead up and roll off, anodization as well as etching followed by dip coating in myristic acid was attempted to create superhydrophobic surfaces. However, the water contact angle on titanium was found to be 148° ± 4°, whereas in the case of 9Cr-1Mo steel, it was 107° ± 2°. A detailed description of the surface-modified superhydrophobic titanium and hydrophobic 9Cr-1Mo steel is presented in this article. The corrosion performance and anti-biofouling properties are ascertained using electrochemical impedance spectroscopy and epifluorescence microscopy. The present study revealed enhanced corrosion resistance and antibiofouling of the materials after superhydrophobic surface modification.

Keywords: Biofouling, corrosion, lotus effect, superhydrophobicity, surface modification.

THE wetting behaviour of solid surfaces by a liquid is a well known aspect of surface chemistry. When a liquid droplet contacts a solid substrate, it will either remain as a droplet or spread out on the surface to form a thin liquid film, a property normally characterized using contact angle (CA) measurements. For a solid substrate, when the CA of water or oil on it is larger than 150°, it is called superhydrophobic or superoleophobic; water or oil drops simply bounce-off the surface. On the other hand, when the CA of water or oil on a surface is almost 0°, it is called superhydrophilic or superoleophilic. Superhydrophobicity is an interesting multidisciplinary topic that covers biology, materials science, chemistry and physics. In nature, the leaves of plants like *Nelumbo nucifera*, *Colocasia esculenta*, *Brassica oleracea*[1–7], the wings of butterflies[8] and the legs of water striders[9] are all superhydrophobic. The lotus leaf appears to have a smooth surface consisting of micro–nano epidermal structures. Moreover, they are often covered with tiny wax crystals of size a few hundred nanometres. The combination of micro and nanostructures, together with a hydrophobic chemistry, generates the phenomenon of superhydrophobicity in lotus leaf with water droplets on such surfaces[10] exhibiting CAs above 150°. Recently, much interest has been directed towards fabrication of biomimetic superhydrophobic surfaces because of their potential applications in self-cleaning glasses, non-wetting clothes, corrosion protection coatings, anti-snow sticking and monument protection[11–13]. In this article, we report the development of superhydrophobic titanium and hydrophobic 9Cr-1Mo steel surfaces by anodization or etching followed by dip coating and show that these surfaces are resistant to corrosion and biofouling.

Microscopic analysis of lotus leaf

A closer microscopic examination of the lotus leaves reveals micro–nanostructures as shown in Figure 1. They have papillose epidermal cells and an additional layer of epicuticular waxes that provide the water repellency. From Figure 1 *a*, it could be inferred that the average height of the papillae varies from 0.2 to 3 μm. Figure 1 *b* shows that the distance between two papillae varies from 8 to 20 μm. Figure 1 *c* shows the approximate diameter of the protrusions varies between 8 and 10 μm. Figure 1 *d* shows the morphology of a single protrusion and the presence of nanocrystal wax pins on the protrusions. It could be inferred from Figure 1 that the centre region of the papillae is denser compared to the periphery of the papillae. In general, the region between the micron-sized papillae is densely packed with nano-sized wax pins. Roughness analysis using AFM indicated that the lotus leaf surface has an average roughness varying from 180 to 750 nm of different textures on the surface. As air is trapped between the micro–nano features, the water drops rest only on the tip of the surface microstructures, thereby minimizing the interfacial area between the surface and the water drops.

Titanium and 9Cr-1Mo steel

Titanium is well known for its good corrosion resistance in general and total immunity towards microbially

*For correspondence. (e-mail: kamachi@igcar.gov.in)

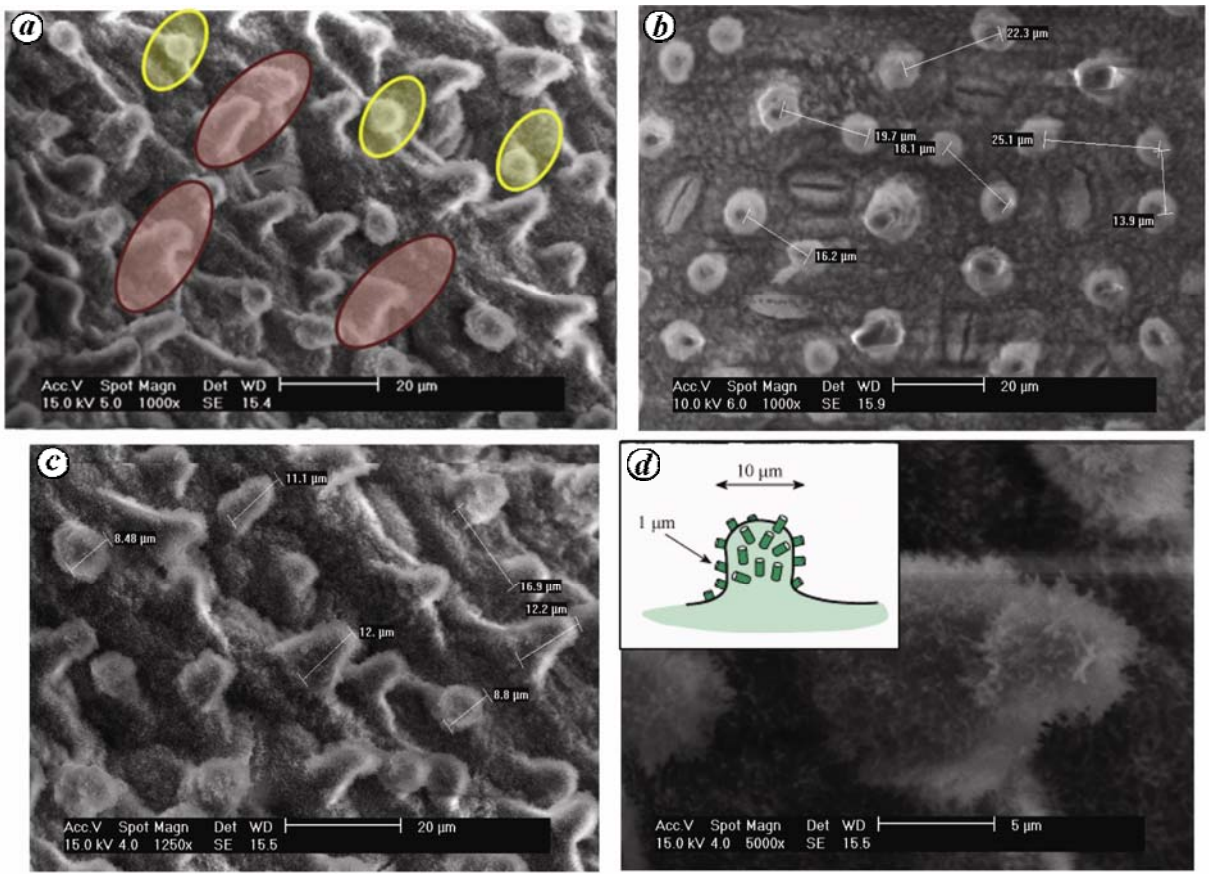

Figure 1. SEM micrograph of lotus leaf indicating (***a***) two different scale papillae, (***b***) the distance between the protrusions, (***c***) the height of the protrusions and (***d***) nanocrystal wax pins on the protrusions. (Inset) Schematic representation of the protrusion with the nanocrystal wax pins.

influenced corrosion in sea-water environment. Titanium is used as condenser material for sea-water applications in nuclear power plants and dissolver vessel in nitric acid (HNO_3) environment of spent nuclear fuel reprocessing plants. There is a constant need to increase the corrosion resistance properties of titanium for prolonged service. But titanium faces an unresolved problem of biofouling in such applications owing to its increased biocompatibility and surface hydrophilicity. Amongst the chrome–moly steels with chromium weight per cent varying from 8 to 12, 9Cr-1Mo steel is extensively used as the structural material in power-generating industries, because of its good combination of mechanical properties and corrosion resistance. However, being a steel the material surface easily forms rust layers during fabrication, storage and service conditions because of its high affinity to moisture, contamination and oxygen. If we can suitably modify the surfaces which can repel the presence of aqueous conditions (moisture, contamination, dissolved oxygen) on the surface of titanium and 9Cr-1Mo steel, then corrosion initiation at the surfaces can be avoided or delayed as the modified surfaces do not provide conditions conducive to initiate corrosion attack. Thus generating a 'superhydrophobic' surface with water repellency is an attractive option to prevent and delay the onset of corrosion processes at the surfaces of engineering components in natural atmosphere. In the present work, superhydrophobic titanium[14] and hydrophobic 9Cr-1Mo steel were obtained by creating micro–nano roughness using anodization/chemical etching followed by dip coating in myristic/stearic acid (hydrophobic coating materials).

Experimental methods

Titanium coupons (Grade-2) of size 30 mm × 20 mm × 3 mm were used for the study. All samples were polished using 80–1000 grade SiC paper. In order to achieve the required surface roughness, which is a prerequisite for better adhesion of the coating materials as well as the initial requirement for a surface to exhibit superhydrophobicity, four different types of surface finishes were prepared: type 1 – anodized, type 2 – anodized and pickled for 2 min, type 3 – polished and subjected to extended pickling for 10 min and type 4 – as polished specimen (up to 1000 grade SiC paper). Triplicate samples for each condition were prepared. Anodization was carried out using cylindrical titanium cathode and the titanium coupon under study as the anode. The electrolyte used for anodization was a mixture of 1 M sulphuric acid (H_2SO_4) and 0.16 M hydrofluoric acid (HF). Anodization was carried out at 30 V for a duration of 1 h. Pickling solution for the samples was prepared using 400 g/l HNO_3

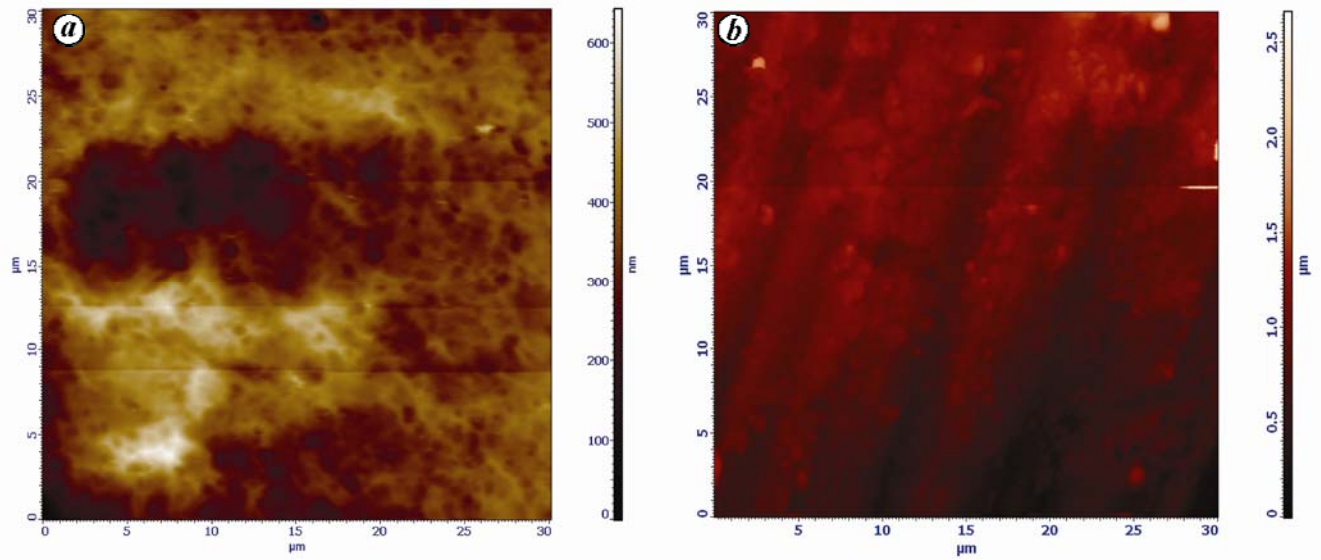

Figure 2. AFM images showing titanium surface coated with myristic acid of different concentrations: (***a***) 0.06 M and (***b***) 0.5 M.

and 40 g/l HF. In order to optimize the concentration of myristic acid, type-4 titanium was dipped for 10 days in different molar solutions (0.06, 0.1, 0.2, 0.3 and 0.5 M) of myristic acid using ethanol as the solvent. The samples with four different surface finishes of titanium were dipped in 0.5 M myristic acid and kept for 10 days at 37°C. After 10 days, the samples were taken out, washed with ethanol and distilled water, and then dried. One sample from each type of surface modification was kept in an oven at 80°C and 130°C in order to stabilize the coating and one set of samples was kept as such at room temperature.

9Cr-1Mo steel coupons of size 10 mm × 10 mm × 10 mm were polished using 80–1000 grade SiC paper. One set of polished samples was etched to modify the surface roughness using ethanol : HNO_3 mixture in the ratio 9 : 1 for 15 s. No etching was carried out for another set of polished samples. Then the samples were ultrasonically cleaned with acetone and washed with distilled water. Two sets of samples were dipped in a conical flask containing 0.5 M myristic acid dissolved in ethanol and the flask was tightly sealed. The set-up was kept at 37°C for about 10 days. After 10 days the samples were taken out and washed with ethanol and distilled water. One sample from each set was kept as such, whereas other samples was heated at 80°C and 110°C for 1 h. A set of 10 samples was etched separately and dipped in 0.5 M myristic acid to analyse the effect of immersion time. During the immersion period of 10 days, one sample was taken out per day and heated at 110°C for 1 h.

Characterization of the superhydrophobic surface

NT–MDT atomic force microscope (Solver Pro EC/ Electrochemical STM/AFM) in contact mode and Philips XL 30 ESEM were used to characterize the surface roughness and particle size. The CAs of the surfaces were measured using a KRUSS DAS 100 contact angle instrument. The stability of the coating in seawater and HNO_3 medium was studied using electrochemical impedance spectroscopy (EIS) conducted in sterile seawater and HNO_3 (0.1, 0.5 and 1 M) using Solartron 1255 frequency response analyser (FRA) and Solartron 1287 electrochemical interface to evaluate the stability of the superhydrophobic coating and its corrosion resistance. All the experiments were carried out in the frequency range from 10^{-1} to 10^5 Hz by superimposing an AC voltage of 10 mV amplitude. An electrochemical polarization cell of three-electrode cell type was used, where the reference electrode was saturated Ag/AgCl, counter electrode was Pt and working electrode was polished/coated titanium sample. Seawater for EIS study was prefiltered using Whatmann No. 1 filter paper for removing macrofoulants. The test samples were stabilized in all the solutions for 30 min before starting the experiment. The superhydrophobic surfaces repelling microbial attachment were studied by exposing these surfaces to seawater and the stained samples were observed under a Nikon Eclipse E600 epifluorescence microscope (excitation filter BP 490; barrier filter O 515).

Microscopic studies

AFM studies of titanium surfaces coated with different concentrations of myristic acid were carried out. The results are shown in Figure 2. AFM images showed smooth and efficient coating on the surface for 0.5 M concentration of myristic acid. The particle size of the coating was in the nanometric range (100–200 nm) compared to the coatings formed using 0.06, 0.1, 0.2 and 0.3 M myristic acid. This is due to more particles getting deposited on

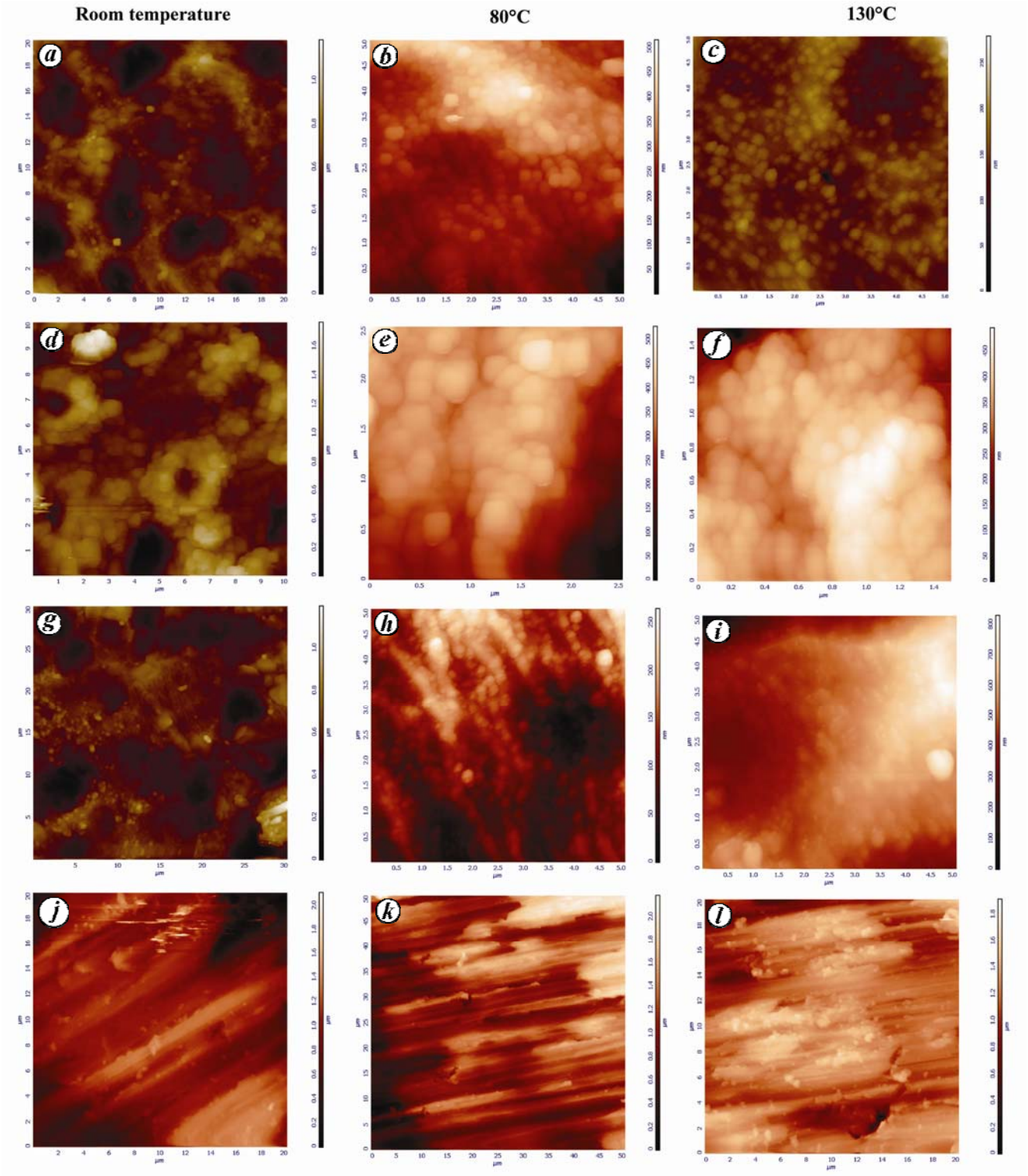

Figure 3. AFM images showing 0.5 M myristic acid coated on titanium: (***a*–*c***) type 1, (***d*–*f***) type 2, (***g*–*i***) type 3 and (***j*–*l***) type 4.

the surface as the concentration increases. Hence 0.5 M concentration of myristic acid was chosen as the optimized concentration for coating titanium samples. AFM-based image analysis (Figure 3) of four types of precoating treatments indicated that type 1 surface showed maximum roughness compared to other surface treatments. Average roughness value mathematically describes the arithmetic average value of the departure of the profile from the centerline throughout the sampling length[15]. The roughness values for type 1 to 4 are 423, 383, 326

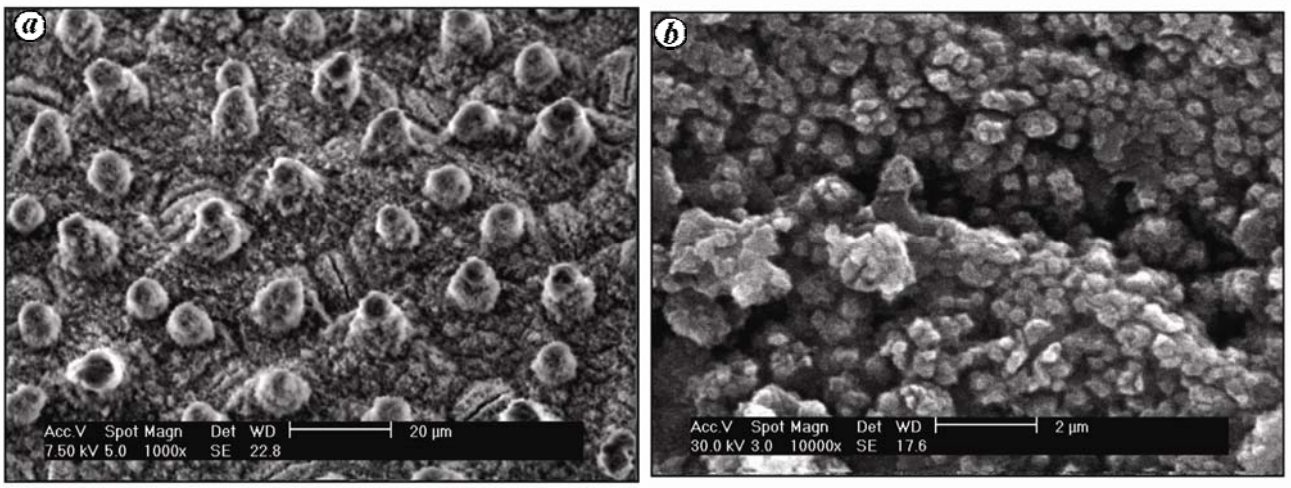

Figure 4. SEM images of (***a***) lotus leaf and (***b***) superhydrophobic titanium surface.

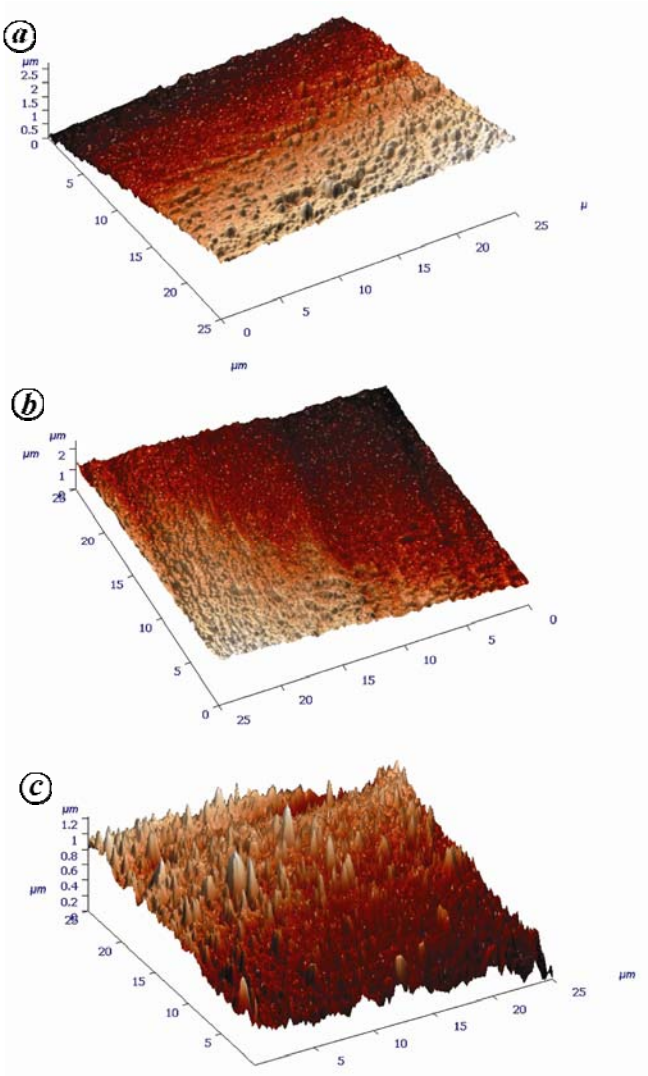

Figure 5. AFM images of 9Cr-1Mo steel (***a***) etched, (***b***) etched and heat treated at 80°C and (***c***) etched and heat treated at 110°C. All the three samples are dip coated in 0.5 M myristic acid.

and 201 nm respectively. Anodization involving oxidizing electrolyte with fluoride ions at pH < 6 usually gives porous oxide film on the surface[16]. Hence the porous layer formed during anodization makes the surface rougher compared to other pretreated surfaces. For type-2 surface, oxide on the surface gets dissolved by pickling for 2 min and hence the templates of oxide layer formed alone remain on the surface, which has considerably less roughness than anodized surface. Type-4 surface with smooth polishing exhibited the lowest roughness value. The study of changes in the surface topography with different immersion times of titanium in HF showed a significant increase of the surface roughness and surface complexity when the exposure time in HF was increased[17]. Hence when the polished surface was pickled for almost 10 min (type 3), the surface was significantly roughened since the pickling bath contains HF which etches the surface and makes the surface rougher than the polished surface. AFM results (Figure 3 *a–c*) showed that the anodized type-1 surface has uniform as well as compact coating compared to other surfaces. The coating was fairly uniform in the case of type 2 (Figure 3 *d–f*), while on type-3 (Figure 3 *g–i*) as well as type-4 (Figure 3 *j–l*) surfaces the coating was not uniform. Type-4 polished titanium surface shows poor adherence of myristic acid coating and the thickness is less as the polishing lines are still visible. As the heat treatment temperature increases, the surface coating morphology also differs marginally, which can be observed from the AFM images. The reason may be the sudden evaporation of ethanol that makes the surface porous and hence there is an increase in roughness.

As discussed earlier, lotus leaf shows superhydrophobicity because of micro–nano protrusions with hydrophobic wax-type of chemical coating over them (Figure 4 *a*). SEM image of myristic acid-coated type-1 titanium surface (Figure 4 *b*) shows rough surface with bunch-like

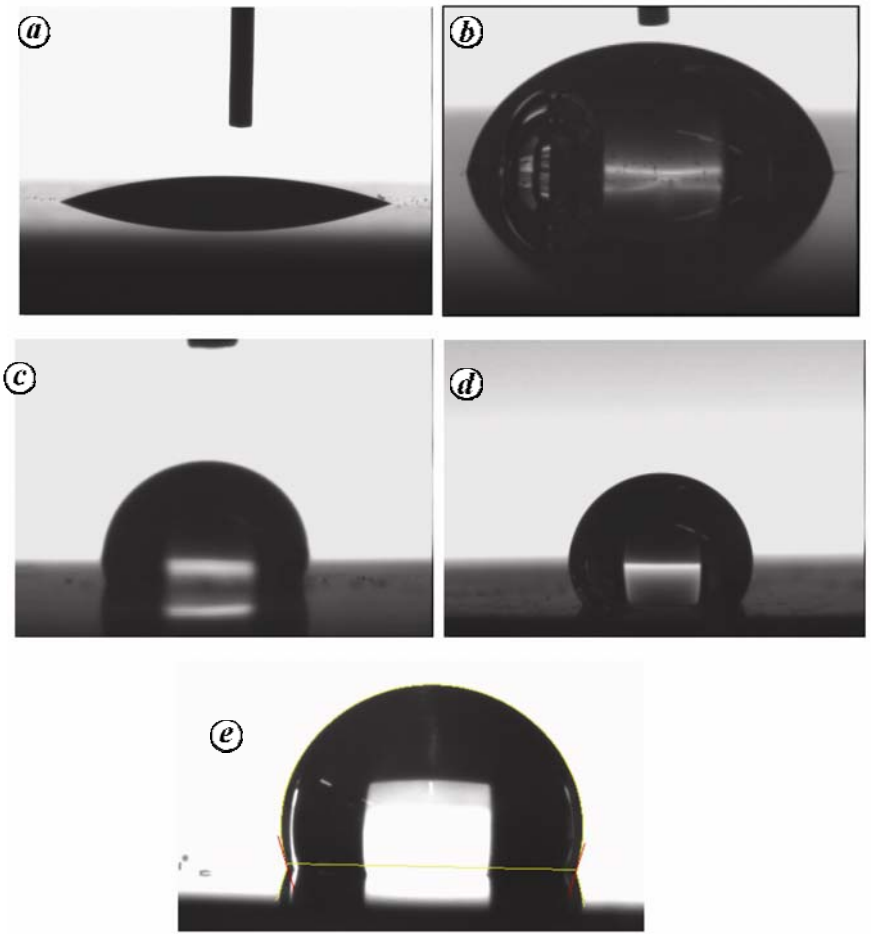

Figure 6. Water droplet on different titanium surface finishes (***a***–***d***) and hydrophobic 9Cr-1Mo steel surface (***e***).

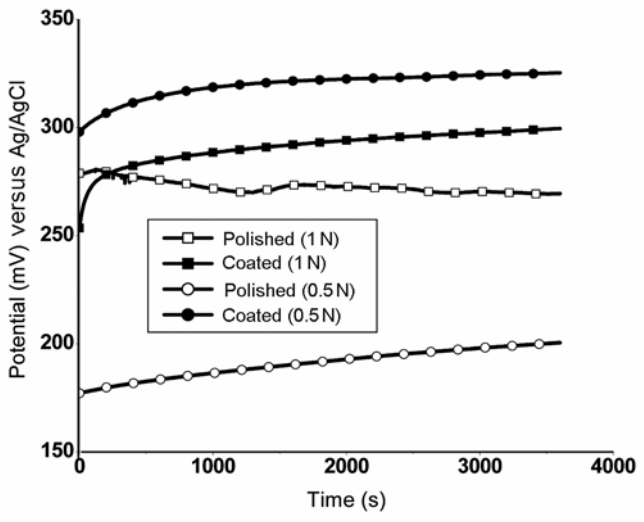

Figure 7. Open circuit potential–time measurements for polished and superhydrophobic surfaces in 0.5 and 1 N nitric acid.

projections, which ultimately increase the effective surface area[18] and enable the titanium surface to give high WCA. It is believed that the gaps between the projections act as valleys[19] where air gets trapped, so that water minimizes its contact area with the surface leading to an increase in the WCA. The 'tail' of the fatty acid is a long hydrocarbon chain, making it hydrophobic, and the 'head' of the molecule is a carboxyl group which is hydrophilic. While coating the fatty acid on the surface, the head (hydrophilic end) gets adhered on the surface leaving the tail (hydrophobic end) upwards, which makes the coated surface hydrophobic.

Hydrophobic surface modification of 9Cr-1Mo steel involves two steps: (i) pretreatment to modify the surface roughness and (ii) dip coating in 0.5 M myristic acid. The increase in surface roughness can be viewed in Figure 5 by comparing the AFM images of as etched samples as well as etched and heat-treated (at 80°C and 110°C respectively) samples. It is reported in the literature[20] that by heating, it is possible to achieve double the CA and significant increase in hydrophobicity. By heating the organic film on metal substrate, it may react with the metal and with itself, and enhance the cross-linking through physical entanglement[21]. Heating also helped in the evaporation of the solvents. All these effects contribute to the compactness of the organic film and improved its hydrophobicity.

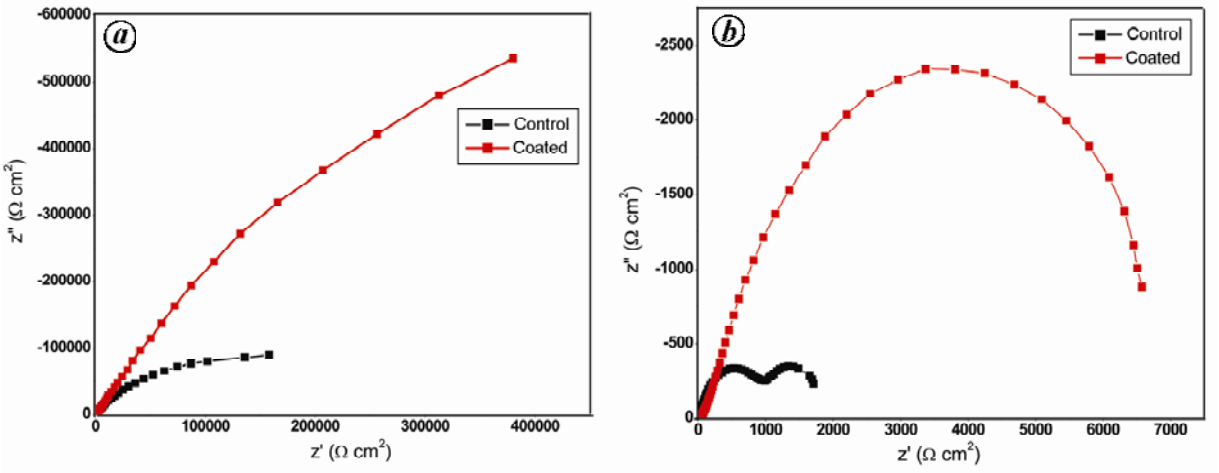

Figure 8. Electrochemical impedance spectra of superhydrophobic and control: (***a***) titanium and (***b***) 9Cr-1Mo steel.

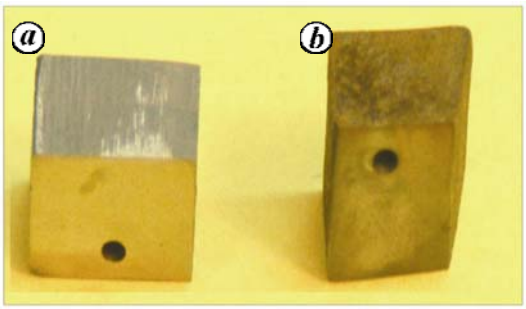

Figure 9. Photograph showing (***a***) absence of corrosion on myristic acid-coated 9Cr-1Mo steel and (***b***) corrosion of uncoated 9Cr-1Mo steel.

CA measurements

Figure 6 *a–d* shows the water droplet on different titanium surface finishes captured on a CCD camera. The results indicate that precoating treatment by anodization in 1 M H_2SO_4 with 0.16 M HF for 1 h at 30 V followed by dip coating in 0.5 M myristic acid for 10 days led to the development of superhydrophobic surfaces with CA of 148° ± 4°. Type 2 (anodized and pickled for 2 min) and type 3 (anodized and pickled for 10 min) showed WCA of 115° ± 3° and 80° ± 6° respectively which are hydrophobic and hydrophilic in nature. Type-4 surface (as polished) showed superhydrophilicity with WCA 26° ± 3°, whereas as received CP grade-2 titanium surface[22] (industrial finish) showed WCA of 53.9° ± 5.1°. These CAs could also be corroborated with the roughness value of the surfaces and the corresponding AFM images (Figures 2 and 3). This confirmed that the CAs were lower for smooth surfaces, while they were higher for rough surfaces. In the case of 9Cr-1Mo steel, the hydrophobic coating was thick and uniform when the sample was immersed in myristic acid for 24 h (WCA 107° ± 2°), as shown in Figure 6 *e*.

Electrochemical studies

Electrochemical studies were conducted on superhydrophobic titanium surfaces and polished titanium was used as control specimen. Variation in open circuit potential (OCP) with time was observed in 0.5 and 1 M HNO_3 for 3600 s. OCP for coated and polished titanium specimens in 0.5 and 1 M HNO_3 showed (Figure 7) nearly noble and steady state. In the case of 0.5 M HNO_3, the OCP shifted significantly to the noble direction for the coated surface compared to the polished one. However, the shift in noble direction for 1 M HNO_3 was not as much as that for 0.5 M HNO_3. The shifting of OCP towards the noble direction indicated greater passivity of the protecting layer on the surface[23].

Nyquist plots (Figure 8 *a*) showed that there was noticeable increase in diameter of the semicircle for coated titanium surface compared to the polished surface. The increase in semicircle radius normally showed an increase in stability of the passive film; also, the increase in charge transfer resistance (R_{ct}) which is inversely proportional to the corrosion rate of the system[24]. The high R_{ct} value of 1.3×10^{11} (Ω cm^2) and low capacitance value of 2.0×10^{-4} (F/Cm^{2}s^{-n}) of coated surfaces indicated that the coating on these surfaces significantly enhanced the corrosion resistance[11,25]. Figure 8 *b* shows the Nyquist plot of 9Cr-1Mo steel in which higher semi arc behaviour indicating increase in the corrosion resistance of the coated surface was noticed compared to as polished sample. The corrosion properties of these coated surfaces in seawater were tested by keeping the uncoated and coated 9Cr-1Mo steel samples in seawater for about 24 h. The results showed that the uncoated steel surfaces corroded with visible accumulation of rust (Figure 9), whereas the coated 9Cr-1Mo steel surface did not show any sign of corrosion. Therefore, it could be inferred that the hydrophobic coating acts as a physical barrier between the metal and environment, leading to increased corrosion

resistance. Hydrophobic coatings of myristic acid on 9Cr-1Mo steel surface stabilized by heating at 110°C showed increased corrosion resistance.

Biofouling studies

Superhydrophobic titanium samples were surface-sterilized using UV–visible light inside a Klenzaids Laminar Air Flow Chamber for 2 h. These samples were then exposed to seawater for about 24 h. Then the samples were rinsed in distilled water, air-dried and flooded using acridine orange (0.1% solution in distilled water). After 5 min, the excess stain was drained-off, and the coupons were rinsed in distilled water and dried in the dark. Acridine orange is a fluorescent dye which differentially stains single-stranded RNA and double-stranded DNA; fluoresces orange when intercalated with the former and green while complexing with the latter[13]. The stained samples observed under a Nikon Eclipse E600 epifluorescence microscope revealed their ability to resist microbial attachment, exhibiting microbe-repelling property (Figure 10). The orange fluorescing cells depict the actively metabolizing cells on the titanium surfaces and the green fluorescing cells represent the inactivated microbial cells.

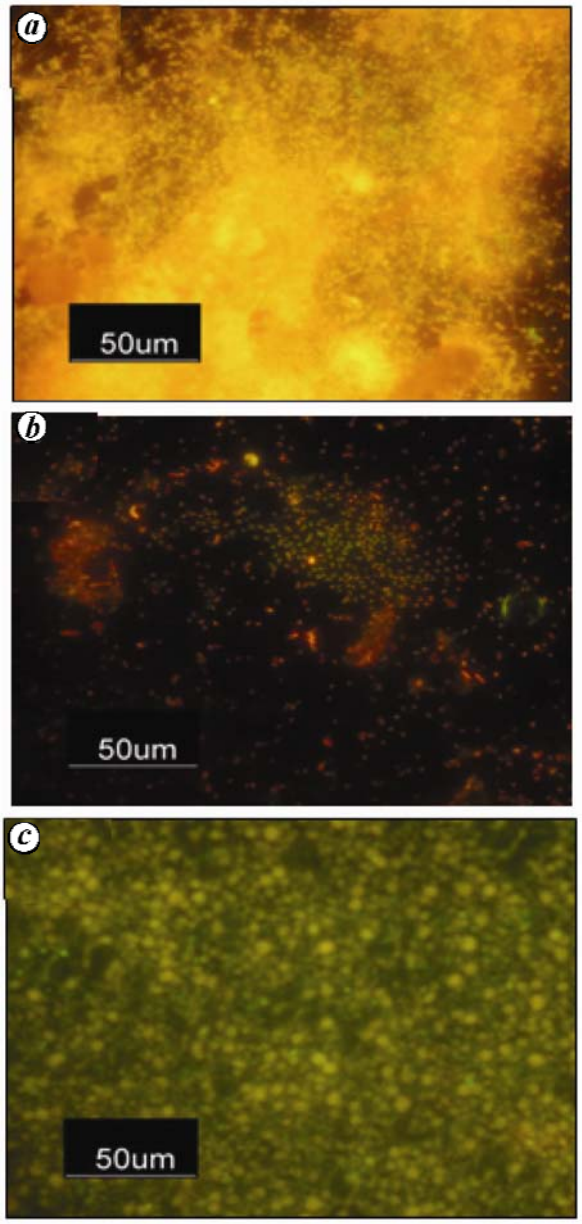

Figure 10. Microbial attachment test. ***a***, Biofilm formation on polished titanium. ***b***, Significant reduction in microbial attachment on hydrophobic titanium. ***c***, No microbial attachment on superhydrophobic titanium surfaces.

Superhydrophobic coatings are reported to lower the surface free energy of a surface[26–28]. *In vivo* studies have confirmed the beneficial effect of a low surface free energy material in controlling microbial adhesion. The lower the surface free energy, the surfaces attracted significantly less microorganisms after 9 days and those attached were insignificantly associated with the surface compared to bacteria adhering on high surface free energy surfaces[29]. Silicone oil-coated enamel, fluorinated ethylene-propylene (FEP)-coated abutments (transmucosal dental implants) and modified silicone rubber voice prosthesis with perfluoroalkylsiloxane have showed significant reduction in biofilm formation[26–28]. All these studies confirmed that the superhydrophobic coatings can effectively control microbial adhesion. However, most of the results reported in the literature indicated reduced microorganism attachment, whereas the present study showed that the superhydrophobic titanium surfaces had 'no or zero microbial attachment'. In contrast, the control sample which is superhydrophilic in nature showed significant biofilm formation and the hydrophobic surface showed significant reduction in biofilm formation.

Conclusions

The results of the present study indicate that precoating treatment by anodization using 1 M H_2SO_4 and 0.16 M HF as electrolyte for 1 h at 30 V followed by dip coating in 0.1 M myristic acid for 10 days led to the development of superhydrophobic titanium surfaces with CAs of 148° ± 4°. In the case of 9Cr-1Mo steel, etching in ethanol and HNO_3 mixture followed by dip coating in 0.1 M myristic acid resulted in a hydrophobic surface with WCA of 107° ± 2°. SEM and AFM images showed uniform coating and the surface was micro–nano rough with cluster-like projections. EIS results showed that the coatings on these surfaces were stable and there was a significant increase in the corrosion resistance of titanium in seawater. The superhydrophobic surfaces of titanium exposed to seawater and observed using an epifluorescence microscope revealed their ability to resist microbial

attachment, exhibiting microbe-repelling property. Hydrophobic 9Cr-1Mo steel immersed in seawater did not show any sign of corrosion. Thus, these results confirm that the surface modification of titanium and 9Cr-1Mo steel lead to the formation of superhydrophobic and hydrophobic surfaces respectively, with good resistance to biofouling and corrosion. Extensive studies are under progress in this direction to study the practical feasibility of implicating this coating technology into real-time applications.

1. Barthlott, W. and Neinhuis, C., Purity of the sacred lotus, or escape from contamination in biological surfaces. *Planta*, 1997, **202**, 1–8.
2. Cheng, Y. T., Rodak, D. E., Angelopoulos, A. and Gacek, T., Microscopic observations of condensation of water on lotus leaves. *Appl. Phys. Lett.*, 2005, **87**, 194112.
3. Choi, C. H., Hagvall, S. H., Wu, B. M., Dunn, J. C. Y., Beygui, R. E. and Kim, C. J., Cell interaction with three-dimensional sharp-tip nanotopography. *Biomaterials*, 2007, **28**, 1672–1679.
4. Neinhuis, C. and Barthlott, W., Characterization and distribution of water repellent, self-cleaning plant surfaces. *Ann. Bot.*, 1997, **79**, 667–677.
5. Koch, K., Neinhuis, C., Ensikat, H. J. and Barthlott, W., Self assembly of epicuticular waxes on living plant surfaces imaged by atomic force microscopy (AFM). *J. Exp. Bot.*, 2004, **55**, 711–718.
6. Karthick, B. and Maheshwari, R., Lotus-inspired nanotechnology applications. *Resonance*, 2008, **13**, 1141–1145.
7. Arvind Singh, R., Yoon, E. S., Kim, H. J., Kim, J., Jeong, H. E. and Suh, K. Y., Replication of surfaces of natural leaves for enhanced micro-scale tribological property. *Mater. Sci. Eng. C*, 2007, **27**, 875–879.
8. Goodwyn, P. P., Maezono, Y., Hosoda, N. and Fujisaki, K., Waterproof and translucent wings at the same time: problems and solutions in butterflies. *Naturwissenschaften*, 2009, **96**, 781–787.
9. Gao, X. and Jiang, L., Water-repellent legs of water striders. *Nature*, 2004, **432**, 36.
10. Spaetha, M. and Barthlott, W., Lotus-effect: biomimetic superhydrophobic surfaces and their application. *Adv. Sci. Technol.*, 2008, **60**, 38–46.
11. Yin, Y., Liu, T., Chen, S., Liu, T. and Cheng, S., Structure stability and corrosion inhibition of super-hydrophobic film on aluminum in seawater. *Appl. Surf. Sci.*, 2008, **255**, 2978–2984.
12. Liu, T., Chen, S., Cheng, S., Tian, J., Chang, X. and Yin, Y., Corrosion behavior of superhydrophobic surface on copper in seawater. *Electrochim. Acta*, 2007, **52**, 8003–8007.
13. Mah, T. C. and Tool, G. A. O., Mechanisms of biofilm resistance to antimicrobial agents. *Trends Microbiol.*, 2001, **9**, 34–39.
14. Mahalakshmi, P. V., Judy Gopal, Kamachi Mudali, U. and Baldev Raj, Development of superhydrophobic titanium surfaces with corrosion and biofouling resistance (submitted to *Surface Engineering*).
15. Subramanian, C., Strafford, K. N., Wilks, T. P., Ward, L. P. and McMillan, W., Influence of substrate roughness on the scratch adhesion of titanium nitride coatings. *Surf. Coat. Technol.*, 1993, **62**, 529–535.
16. Baun, W. L., Formation of porous films on titanium alloys by anodization. *Surf. Technol.*, 1980, **11**, 421–430.
17. Lamolle, S. F., Monjo, M., Rubert, M., Haugen, H. J., Lyngstadaas, S. P. and Ellingsen, J. E., The effect of hydrofluoric acid treatment of titanium surface on nanostructural and chemical changes and the growth of MC3T3-E1 cells. *Biomaterials*, 2009, **30**, 736–742.
18. Bhagat, S. D., Kim, Y. H. and Ahn, Y. S., Room temperature synthesis of water repellent silica coatings by the dip coat technique. *Appl. Surf. Sci.*, 2006, **253**, 2217–2221.
19. Satyaprasad, A., Jain, V. and Nema, S. K., Deposition of superhydrophobic nanostructured Teflon-like coating using expanding plasma arc. *Appl. Surf. Sci.*, 2007, **253**, 5462–5466.
20. Zhang, J., Development of environmentally friendly non-chrome conversion coatings for cold-rolled steel, Ph D dissertation, 2003.
21. Guo, Z., Zhou, F., Hao, J. and Liu, W., Effects of system parameters on making aluminum alloy lotus. *J. Colloid Interf. Sci.*, 2006, **303**, 298–305.
22. Ponsonnet, L., Reybier, K., Jaffrezic, N., Comte, V., Lagneaub, C., Lissac, M. and Martelet. C., Relationship between surface properties (roughness, wettability) of titanium and titanium alloys and cell behaviour. *Mater. Sci. Eng. C*, 2003, **23**, 551–560.
23. Padhy, N., Kamal, S., Chandra, R., Kamachi Mudali, U. and Baldev Raj, Corrosion performance of TiO_2 coated type 304L stainless steel in nitric acid medium. *Surf. Coat. Technol.*, 2010, **204**, 2782–2788.
24. Bairi, L. R., Ningshen, S., Kamachi Mudali, U. and Baldev Raj, Microstructural analysis and corrosion behaviour of D9 stainless steel – zirconium metal waste form alloys. *Corros. Sci.*, 2010, **52**, 2291–2302.
25. Liu, T., Yin, Y., Chen, S., Chang, X. and Cheng, S., Superhydrophobic surfaces improve corrosion resistance of copper in seawater. *Electrochim. Acta*, 2007, **52**, 3709–3713.
26. Rolla, G., Ellingsen, J. E. and Herlofson, B., Enhancement and inhibition of dental plaque formation – some old and new concepts. *Biofouling*, 1991, **3**, 175–181.
27. Quirynen, M., Van der Mei, H. C., Bollen, C. L., Geertsema-Doornbusch, G. I., Busscher, H. J. and Van Steenberghe, D., Clinical relevance of the influence of surface free energy and roughness on the supragingival and subgingival plaque formation in man. *Colloid Surf. B*, 1994, **2**, 25–31.
28. Everaert, E. P. J. M., Mahieu, H. F., Van de Belt-Gritter, B., Peeters, A. J. G. E., Verkerke, G. J., Van der Mei, H. C. and Busscher, H. J., Biofilm formation *in vivo* on perfluoro–alkylsiloxane–modified voice prostheses. *Arch. Otolaryngol. Head Neck Surg.*, 1999, **125**, 1329–1332.
29. Quirynen, M., Marechal, M., Busscher, H. J., Weerkamp, A., Arends, J. and Darius, P. L., The influence of surface free-energy on planimetric plaque growth in man. *J. Dent. Res.*, 1989, **68**, 796–799.

Received 20 May 2011; revised accepted 4 October 2011